Application of Artificial Neural Networks for Direct Detection of Microcalcification Clusters in Digital Mammograms

Thierry-Pascal Baum
Orly, France

Computer-aided diagnosis (CAD) schemes for the detection of microcalcification clusters (MCCs) come in two types: indirect and direct. Indirect detection of MCCs detect individual microcalcifications first, which are then used to detect clusters. Direct detection detects clusters in a unique step, without any previous detection of individual microcalcifications. Nearly all the existing literature describes indirect detection. In this study, we investigated a direct detection scheme. We divided digital mammograms into regions of interest (ROIs) and computed a set of parameters on each ROI. We discriminated parameters through an artificial neural network (ANN) that gave the presence or absence of an MCC in the examined ROI. Final images with suspicious ROIs containing MCCs were shown to radiologists. Results appeared to be interesting enough to compete with indirect detections. Extra studies could prove direct detection to be a better approach as compared to indirect detection CAD schemes.

Keywords: breast cancer, digital mammography, mammograms, artificial neural networks, direct detection, indirect detection, clusters of microcalcifications, computer-aided diagnosis.

Introduction

At present, breast cancer is a major public health problem and is the leading cause of cancer and the second cause of death in Europe (Le code Européen 95). In western countries, about one out of 10 women will develop breast cancer in their lifetime. With ageing population, statistics are getting worse as shown by the progression of breast cancer in woman lifespan in the United States: 1 out of 20 women in 1940, 1 out of 14 in 1960, 1 out of 11 in 1980 (Hoffman et al 94) and 1 out of 8 in 1993 (Winfield et al 94).

Early diagnosis is the most important factor in mortality reduction (Feig 93). The best way to provide the earliest diagnosis is systematic mass screening by mammography. Such a screening, if applied in good conditions and generalized to all the population, would allow a decrease of 30% in breast cancer mortality (Wald et al 94, Cuckle 91). Mammography allows the detection of very early signs of breast cancer, one of the major signs being clusters of microcalcifications (MCCs).

Computer-aided diagnosis (CAD) may contribute to solve some of the problems raised by mass screening in breast cancer detection. Several studies have shown that missed lesions could be reduced by half when radiologists were given computer prompts with regard to possible abnormalities (Vyborny 94, Kegelmeyer et al 94, Chan et al 90), and that artificial intelligence techniques could provide a correct benign to malignant classification ratio that is more efficient than the one given by general radiologists not specialized in mammographic reading (Vyborny 94, Getty et al 88, Wu et al 93).

In this study, we developed a CAD scheme to help radiologists in mass screening of breast cancer by prompting them for MCCs. Nearly all the teams publishing about MCCs detection use an indirect scheme (Chan et al 90, Davies et al 90, Chan et al 87, Clarke et al 94, Fam et al 88, Bankman et al 91, Bankman et al 93, Stafford et al 93, Nishikawa et al 93, Nishikawa et al 95, Karssemeijer et al 92, Qian et al 95) and realize their detections by first detecting individual microcalcifications, and then use these previously detected microcalcifications to detect the

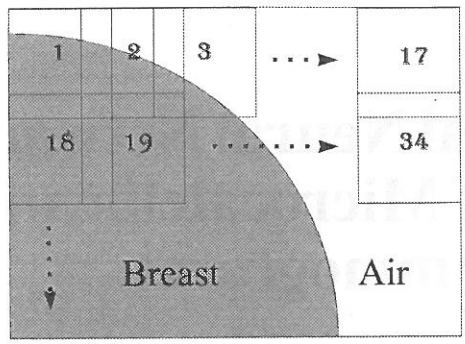

Fig. 1. Progression of ROIs with partial overlapping over a half mammogram.

clusters. In this study, we have not detected individual microcalcifications, but we have realized a direct detection of clusters, without using previously detected microcalcifications. We wanted to avoid adverse effects inherent to indirect detections, the numerous false positive microcalcifications detected by this type of schemes (Baum 97a, Baum 97b).

Material

Mammograms

The 50 mammograms used for this study were obtained from the Curie Institute in Paris and have been selected by expert mammographers as being particularly difficult and subtle to diagnose. Cases were selected among patients who had undergone a biopsy with X-ray and an histologic examination of the removed tissue to confirm the existence of the MCCs detected by mammographers.

Digitization of Mammograms

All mammograms were acquired with the dedicated mammographic system UM Philips Mammodiagnos at 28 kV. A Kodak ortho MA mammographic film was used.

The films were digitized on a rectangular surface containing all of the breast tissue and its close surroundings (air). The spatial resolution was 50 μm/pixel and the quantification was 8 bits/pixel allowing a dynamic range of 256 grey levels on a CCD scanner. The average size of the resulting digital images was 3000 $\times$ 1500 pixels.

Methods

Extraction of Parameters

A set of parameters was computed to characterize clusters of microcalcifications and was used as input in the neural network for discrimination.

Digital images were processed by 128 $\times$ 128 pixels regions of interest (ROIs). ROIs were taken all over the image with a step of 96 pixels (representing a 32 pixels overlapping) for width and height (Figure 1).

Twenty four parameters were computed on each ROI: Fourier transform (10 parameters), Hu moments (7 parameters), granulometry (6 parameters), variance (1 parameter). Each of the 24 parameters was entered in a neural network with 24 input cells to discriminate between two classes: presence or absence of a cluster of microcalcifications in the ROI analyzed. Thus, instead of directly pointing to a cluster, we indicated one or several areas (ROIs) containing a potential cluster of microcalcifications.

Choice of methods

Our aim was to detect an MCC in a ROI. To do this, we had several possibilities. When we looked at MCCs, we could see them in different presentations: a cluster in the centre of the ROI; shifted somewhere in that ROI; a large or a small cluster; or a cluster with different orientations. To simplify the problem, we can reduce the wide variety of cluster presentations in ROIs by utilizing parameters coming from mathematical methods that are invariant to transformations such as translation, rotation or scaling. Image analysis provides some of these descriptors. We chose four of them, belonging to three different domains: frequency domain (FFT), mathematical morphology domain (granulometry), and statistical domain (Hu moments, variance).

Fourier parameters

The Fast Fourier Transform (FFT) is an algorithm that computes the Fourier transform, defined in a continuous space, to a discrete space like a digital image. We used two properties of the FFT:

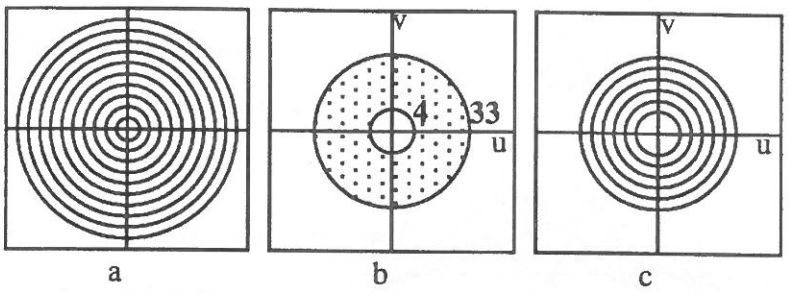

Fig. 2. FFT magnitude invariance: (a) concentric bands, (b) virtual band with inner radius of 4, and outer radius of 33 pixels, (c) virtual band divided into 10 sub-bands.

– shifting invariance: when an object is translated within an image, the FFT magnitude of that image does not change;

– rotation invariance in specific conditions: rotating an object with an α angle within an image will produce the same α angle rotation in the Fourier transform magnitude. Rotation invariance can be obtained if we divide the Fourier spectrum representation space into concentric bands (Figure 2a). Thus, we can compute the energy within each band and obtain a texture description that is invariant to rotation.

The analysis of energy bands shows MCCs in a specific range of frequencies. When FFT is centered in a 128×128 pixels ROI, this range corresponds to a virtual band having an internal radius of 4 pixels and an external radius of 33 pixels (Figure 2b). In this study, we divided this virtual band into ten 3-pixels wide sub-bands (Figure 3c). On each of these ten sub-bands, we computed the mean energy per pixel (sum of grey levels divided by the number of pixels). These 10 energies constituted 10 parameters related to FFT.

Hu moments parameters

An image may be described by its outline or by the part inside the outline. Hu moments belong to methods allowing the description of a region by its inner part, implying a thickness different from zero (e.g. the line has a null thickness, then it cannot be described by Hu moments (Rauber et al 94)). MCCs have a thickness different from zero.

We considered an image f represented by a matrix (x, y) where x and y were the coordinates of a pixel and $f(x, y)$ was the grey level of that pixel.

The definition of a $p + q$ order moment m_{pq} for the image f is:

$$m_{pq} = \sum_x \sum_y x^p y^q f(x, y), \quad p, q = 0, 1, 2, \ldots$$

From the centered and normalized order 2 and 3 moments, Hu extracted 7 moments, invariants for translation, rotation and scaling (Hu 62, Gonzalez et al 92). We used these 7 moments as 7 additional parameters.

Granulometry parameters

The principle of mathematical morphology is to compare an unknown structure (e.g. image to be studied) to a set of forms, the structuring elements, for which all the characteristics (form, size) are known (Schmitt et al 94).

Granulometry is a branch of mathematical morphology. Granulometry filters particles of a determined size in an image (Gonzalez et al 92). For this filtering we used an operation called opening, described in (Schmitt et al 94).

When a structuring element is applied to an image containing particles of different sizes, those particles which do not contain the structuring element, will disappear. Then, it is possible to "sift" an image by using an opening with structuring elements of increasing sizes.

In our study, microcalcifications were assimilated to particles. When the structuring element size was larger than the size of microcalcifications, these were eliminated from the image as were all the other objects having a size under or equal to that of the microcalcifications.

If we consider an image as an horizontal plane and grey levels as an "altitude", the representation of a grey-level image becomes three-dimensional, and the grey-level sum of all the

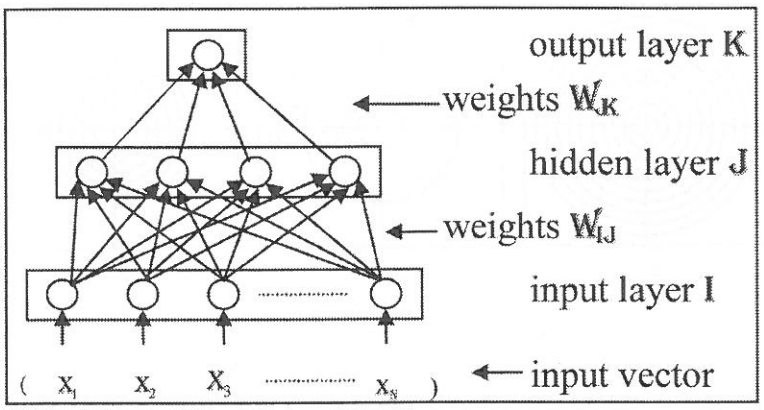

Fig. 3. Multi-layer perception (MLP) used. Nodes (circles) are organized in layers. All nodes from one layer are connected to all nodes in the following layer. Forward propagation is from input to output layer.

pixels of an image will be called the "volume" of that image.

Morphological opening of an image f, noted f_{B_R}, applied with structuring elements having an increasing size R, progressively suppresses the very subtle structures like noise, and at a later stage, microcalcifications. If we substract from the initial image f the image f_{B_R} resulting from the opening, the new image obtained reveals microcalcifications for some specific values of R. If we take the mean volume $m(R)$ (sum of grey levels divided by the number n of pixels) of the new image, R varying from 1 to 6, we can extract 6 granulometry-related $m(R)$ parameters according to the following equation:

$$m(R) = \frac{\text{volume}(f - f_{B_R})}{n}$$
$$R = 1, \ldots, 6; \quad n = \text{number of pixels.}$$

These parameters are invariant for translation and rotation, but not for scaling.

Variance parameter

One of the characteristics allowing radiologists to visually detect an MCC is the cluster contrast from the surrounding tissue. Grey-level variance is a measure of the contrast of an image. Variance is easily computed and invariant for translation, rotation and scaling. It was used as the last parameter.

Artificial Neural Network

Choice

In order to establish a discrimination between the 24 parameters, we chose a multi-layer perceptron (MLP) neural network for the following reasons:

– absence of a model sufficiently precise for our needs. The huge variation of the images to be analyzed, including normal and abnormal breast tissues has precluded, until now, any team from building a model which would take into account the diversity encountered. Thus, a learning method more appropriate than a conventional algorithm has been considered, taking into account the following;

– the nature of the problem to solve suggests a highly non-linear problem for which standard techniques of statistical analysis are very complex to use. By contrast, neural networks are very easy to use with such a non-linear problem;

– absence of strong assumptions concerning the shapes of underlying distributions. For example, when we use neural networks, the distribution of data is not assumed to be Gaussian. Thus, neural networks prove to be more robust when distributions are generated by non-linear processes and are strongly non- gaussian (Lippmann 87).

Architecture

The topology of the net is a multi-layer perceptron (MLP) feed-forward network.

We use a 3-layer perceptron since we can form, with this number of layers, arbitrarily complex decision regions and can separate meshed classes. Such an MLP can form regions as complex as those formed with mixed distributions and nearest-neighbor classifiers (Lippmann 87).

The first layer, or input layer, had 24 nodes for each of the 24 parameters. All input nodes were fully connected to the hidden layer nodes.

The second layer, or hidden layer, had 4 nodes fully connected to the output layer. The number of hidden nodes was determined by repeated trials.

The third layer, or output layer, had a unique node to discriminate between two classes: the presence or the absence of a cluster of microcalcifications in the ROIs to be examined. The output was a continuous value between 0 and 1, and could be seen as the estimation of the probability to have a cluster (conditionally to the observation of the 24 parameters presented as input).

Learning

All weights were initialized to small random values. Weight adaptation was done by applying the standard error back propagation (EBP) algorithm in five steps (Lippmann 87):

All node offsets were initialized to small random values between -0.1 and $+0.1$. For all nodes, we used a sigmoidal non-linearity given by the equation:

$$f(\alpha) = \frac{1}{1 + e^{-(\alpha - \theta)}}.$$

General Algorithm

We began to digitize mammograms on their complete area containing breast tissue and its close surroundings. On these full size digitized mammograms, we extracted ROIs as previously described. The choice of the size of ROIs was determined by two constraints. The first one was the ROI size that should be close to an MCC size (1 cm^2) (Chan et al 87, Fam et al 88, Sickles 86, Freundlich et al 89, de Lafontan et al 94, Lamarque et al 94) but should not exceed that size, which has a maximum of 200×200 pixels with the chosen resolution of 50 μm/pixel. The second constraint was related to the optimization of FFT calculus for which width and height of ROIs should be a power of two. Thus, the closest ROI size was set to 128×128 pixels (0.64×0.64 cm). All processings were calculated on each ROI. The study was segmented into two phases, learning and testing.

The learning phase started with the creation of the learning database (LDB). The LDB was made of 190 ROIs containing an MCC and 340 ROIs containing no MCC. Among the 50 initial images, 24 were reserved for learning. Learning ROIs were selected by an expert mammographer among these 24 mammograms. Then, 24 parameters were computed for each of these ROIs, normalized, and served as input in the MLP. The desired output was 1 for a ROI containing an MCC and 0 for a ROI containing no MCC. After learning, values of the MLP (weights) were kept for later use in the test phase.

The test phase began after the learning phase was completed, and underwent a similar course. The 26 remaining mammograms forming the test database (TDB) were segmented in ROIs on the entirety of their surface, leading to hundreds of ROIs per test mammogram. The 24 parameters were computed on each of these ROIs, and normalized. Parameters entered as input in the MLP gave, for each ROI, a continuously valued output between 0 and 1, depending on the presence of a "full" MCC, a "partial" MCC or the absence of MCC. We considered that a ROI was containing an MCC when the corresponding output was above or equal to 0.5. This threshold was experimentally determined to have approximately the performance of a radiologist under mass screening conditions, that is to say about 70% of correct detection [Holland 82, Kimme-Smith 92]. The location of a ROI containing an MCC was pointed, in the displayed mammogram, in the computer screen. Contiguous ROIs containing an MCC delimited an area containing a "complete" MCC, constituted of several "partial" MCCs.

Upon termination, automated detection of "complete" clusters was compared to the detection by a radiologist expert in mammographic reading.

Results

The performance of our fully automated direct detection scheme was evaluated with the 26 mammograms from the TDB. Each of these mammograms contained one or two MCCs representing an overall number of 30 MCCs. All these MCCs were qualified by experts as being "difficult" or "very difficult" to detect. 540 ROIs were used for the LDB composed of 190 ROIs with MCCs and 340 ROIs containing no MCCs. 11472 ROIs were automatically extracted from digital mammograms belonging to TDB.

Results are given in two forms:

– a form compatible with direct detection;

– a form compatible with indirect detection.

Since direct detections used ROIs to compute all their processings, results are given in terms of the ROIs containing:

– an MCC and being correctly detected = true positive MCC (TP MCC);

– no MCC and being detected as containing an MCC = false positive MCC (FP MCC).

Then, among the 30 existing MCCs, if we look at the FP ratio for a TP ratio of 70% (that is, 21 MCCs correctly detected among 30), the FP ratio from our algorithm was 60 FP ROIs out of a total number of 11472 ROIs analyzed. The FP ratio is then 0.52% (see Table 1).

For comparison purposes with indirect detections (as far as we can compare them), our results were also expressed in terms of FP MCCs per mammogram. Since we obtained 60 FP ROIs out of 26 mammograms, we had an average of 2.3 FP ROIs per mammogram.

Discussion and Conclusion

One of the main difficulties in the detection of MCCs is the high similarity between the signal to detect (MCCs) and the surrounding tissue, both spatially and in frequency. If one does not want to miss a potential cancer, a very sensitive detection is needed, and then a high number of objects close in aspect to microcalcifications, but that are not useful, will be detected at the same time.

In indirect detection, the first thing which is done is to detect all the individual microcalcifications. It is during this first step that one encounters the main problem of this type of detection. If one wants to detect all the existing individual microcalcifications (that is, a high sensitivity), one detects at the same time a large amount of undesired objects (that is, a low specificity) that we call false positives (FPs). The difficulty is to find a way to eliminate all these FPs. After several processes to eliminate FPs, clustering criteria are applied to determine if the remaining microcalcifications can form an MCC. The problem is at the level of FP microcalcifications that are close enough to each other to form a cluster that will be a FP MCC.

To avoid such an adverse effect, we chose direct detection. In this type of scheme, we do not rely on previous detection of individual microcalcifications, that is to say on potential "errors" due to FPs inherent to the indirect detection scheme. The difficulty in direct detection is to find a way to describe the clusters in such a way that is truly representative.

	Wu et al. 92	**Our study**
Resolution	0.1 μm/pixel	0.05 μm/pixel
Dynamic	10 bits/pixel	8 bits/pixel
Number of mammograms	34	50
ROI number for learning	56	540
ROI number for testing	56	11 472
Size of ROIs	3.2×3.2 mm^2	1.08×1.08 cm^2
True positive ROIs	70%	70%
False positive ROIs	20%	0.52%
Type of direct detection	image pixels	parameters

Table 1. Comparative chart for the two direct detections.

We differentiate between two types of direct detection that can be used alone or in combination:

- use of image pixels, directly or after processing;

- use of parameters calculated from image pixels.

In this study, we chose a direct detection CAD scheme using parameters calculated from image pixels.

In literature, we found only one other team that used a direct approach (Wu et al 92). In their study, they tried to detect both individual microcalcifications and MCCs. We considered only the part related to MCCs. The test was performed with 20 combinations of randomly selected training and testing ROI pairs from the database. Pixels of ROIs were used in two neural networks. The networks were able to detect clusters in the frequency domain, but not in the spatial domain. Frequency domain detection gave 20% of FP MCCs for 70% of TP MCCs detected (see Table 1).

If we compare our results to those of (Wu et al 92), we observe a dramatic decrease in FP MCCs since for 70% of TP MCCs we had only 0.52% of FP MCCs (compared to 20%). It is difficult to draw a conclusion, since the reason of these results is probably multifactorial as both studies were conducted on different databases.

Nevertheless, we think that two explanations may be relevant: the representativity of databases and the appropriate choice of parameters to describe MCCs.

In their study, they used a small number of ROIs for learning and testing. We know that, to be useful, the databases must be representative of the problem to be solved. To be representative, one must choose a high number of ROIs to take into consideration the high variety of visual aspects of the normal breast tissue and types of clusters. We tried to take a large training database, but this one has to be selected manually by an expert, to include representative areas. This is a very tedious and time consuming task to accomplish and could be one of the reasons why databases are small. Accordingly, the initial set of mammograms is also very important.

Another problem is to find parameters that can describe and differentiate MCCs from the surrounding breast tissue. It seems there is no theory to solve this problem, and various studies did not show a clear superiority of one of the methods over the others. Our approach wanted to address two problems: reduction of the high diversity, and then the complexity of visual presentations of ROIs; and the compensation for the probably insufficient diversity of databases. For that purpose and in order to describe MCCs on these databases, we found it appropriate to use methods that are invariant to geometrical transforms that MCCs can present, such as translation, rotation and scaling.

Concerning indirect detection, even though the methodology is different, a comparison with direct detection is possible if we use the results in literature as the number of TP MCCs per mammogram, which is not always possible to do. As mentioned for direct detection, the same restrictions apply to the comparison of results since data sets were different in all studies. Our detection is roughly within the range of performance of indirect detection, but seems inferior to the best indirect detection schemes which detect about 1 FP MCC per mammogram for 85% of MCCs.

In this study, our aim was to use direct detection of MCCs instead of indirect detection in order to see if it was possible to avoid the adverse effects related to indirect detection CAD schemes and to obtain a very low percentage of FPs.

Results show that we achieved our goal since 11412 ROIs out of 11472 have been correctly classified, giving a correct discrimination above 99%, and performance of our algorithm is still increasing as we are increasing the learning database, qualitatively and quantitatively. The direct detection approach is then more than viable and is even competitive, compared to indirect detection.

The scanner available at the time of our study was an 8 bit/pixel scanner, since the availability of a dedicated 12 bit/pixel scanner especially designed and under construction for that purpose was delayed. Experiments will be conducted with the 12 bit/pixel scanner as soon as available and will permit a comparison to see if there really is an increase in performance compared to an 8 bit/pixel scanner.

If we want a daily use in clinical practice, further studies are needed since the results are still neither sufficient nor reliable enough.

Acknowledgments The author is grateful to the Curie Institute in Paris for providing mammograms for this study, and to Véronique Baum-Parmentier for providing her useful contribution to the English translation of this article.

References

I. N. BANKMAN ET AL, (1991) An algorithm for early breast cancer detection in mammograms, Presented at the Fifth Annual IEEE Symposium on Computer-Based Medical Systems, Session 6A–B: Frontiers in Detection of Cancer, 362–9.

I. N. BANKMAN ET AL, (1993) Automated recognition of microcalcification clusters in mammograms, Presented at the Proceedings SPIE 93, 1905, 731–738.

T. P. BAUM, (1997a) Artificial neural networks for merging different methods in computer assisted diagnosis in breast cancer, World Congress on Medical Physics and Biomedical Engineering, Nice, France, 35(2), 706.

T. P. BAUM, (1997b) Aide ŕ la détection des foyers de microcalcifications dans le cadre des compagnes de dépistage du cancer du sein, thëse pour le Diplôme de Docteur ës Sciences, Univwrsité Pierre et Marie Curie, Paris VI.

H. P. CHAN ET AL, (1987) Image feature analysis and computer-aided diagnosis in digital radiography, 1. Automated detection of microcalcifications in mammography, Medical Physics, 14 (4): 538–48.

H. P. CHAN ET AL, (1990) Improvement in radiologists' detection of clustered microcalcifications on mammograms: the potential of computer-aided diagnosis. Investigative Radiology, 25, 1102–10.

L. P. CLARKE ET AL, (1994) Tree-structured non-linear filter and wavelet transform for microcalcification segmentation in digital mammography, Cancer Letters, 77, 173–181.

H. CUCKLE, (1991) Breast screening by mammography: an overview, Clinical Radiology, 43, 77–80.

D. H. DAVIES AND D. R. DANCE, (1990) Automatic computer detection of clustered calcifications in digital mammograms, Phys. Med. Biol., 35 (8), 1111–8.

B. DE LAFONTAN ET AL, (1994) Isolated clustered microcalcifications: diagnostic value of mammography — series of 400 cases with surgical verification, Radiology, 190, 479–83.

B. W. FAM ET AL, (1988) Algorithm for the detection of fine clustered calcifications on film mammograms, Radiology, 169 (2), 333–7.

S. A. FEIG, (1993) Mammographic screening: a historical perspective, Seminars in Roentgenology, 28 (3), 193–203.

M. FREUNDLICH ET AL, (1989) Computer-assisted analysis of mammographic clustered calcifications, Clinical Radiology, 40 (3), 295–8.

D. J. GETTY ET AL, (1988) Enhanced interpretation of diagnostic images, Investigative Radiology, 23, 240–252.

R. C. GONZALEZ AND R. E. WOODS, (1992) Morphology In: Digital Image Processing, Addison–Wesley, Massachussetts. ISBN 0–201–60078–1.

F. A. HOFFMAN ET AL, (1994) The mammography quality standards act of 1992, American Family Physician, 49 (8), 1965–1970.

R. HOLLAND ET AL, (1982) So-called interval cancers of the breast, Cancer, 49, 2527–2533.

M. K. HU, (1962) Visual pattern recognition by moment invariants, IRE Transactions on Information Theory, 179–87.

N. KARSSEMEIJER, (1992) Stochastic model for automated detection of calcifications in digital mammograms (1992) Image and Vision Computing, 10 (6), 369–375.

W. P. KEGELMEYER ET AL, (1994) Computer-aided mammographic screening for spiculated lesions, Radiology, 191, 331–337.

C. KIMME-SMITH, (1992) National Cancer Institute Breast Imaging Workshop, Sept 91. AJR, 158, 268.

J. L. LAMARQUE ET AL, (1994) La mammographie initiale peut-elle orienter vers un traitement conservateur? Le Sein, 4 (1), 13–21.

LE CODE EUROPÉEN CONTRE LE CANCER — Un outil destiné aux médecins généralistes — Edition pour la France (1995) Office des publications officielles des Communautés Européennes, Luxembourg, ISBN 92–827–4589–9.

R. P. LIPPMANN, (1987) An introduction to computing with neural nets, IEEE ASSP Magazine, 4–22.

R. M. NISHIKAWA ET AL, (1993) Computer-aided detection and diagnosis of masses and clustered microcalcifications from digital mammograms, Presented at the Proceedings SPIE 93, 1905, 422–32.

R. M. NISHIKAWA ET AL, (1995) Computer-aided detection of clustered microcalcifications on digital mammograms. Medical & Biological Engineering & Computing, 33, 174–78.

W. QIAN ET AL, (1995) Tree-structured wavelet transform segmentation of microcalcifications in digital mammography, Medical Physics., 22(8), 1247–1254.

T. W. RAUBER, (1994) Two dimensional shape description, Technical report from Inductive Pattern Classification, -Methods-Features-Sensors, Ph.D. Thesis, Universidade Nova de Lisboa, Faculdade de Ciências e Tecnologia, Lisboa, Portugal, 5–7.

M. SCHMITT AND J. MATTIOLI, (1994) Mesures Morphologiques In: Morphologie Mathématique, Masson, Paris, Milan, Barcelone, ISBN 2–225–84385–6.

E. A. SICKLES, (1986) Breast calcifications: mammographic evaluation, Radiology, 160, 289–93.

R. G. STAFFORD ET AL, (1993) Application of neural networks to computer aided pathology detection in mammography. Presented at the Proceedings SPIE 93, 1896, 341–52.

C. J. VYBORNY, (1994) Can computers help radiologists read mammograms?, Radiology, 191, 315–317.

N. J. WALD ET AL, (1994) European Society of Mastology Consensus Conference on Breast Cancer Screening: Report of the Evaluation Committee, The British Journal of Radiology, 67 (802), 925–933.

D. WINFIELD ET AL, (1994) Technology transfer in digital mammography: report of the joint National Cancer Institute-National Aeronautics and Space Administration Workshop of May 19–20, 1993, Investigative Radiology, 4, 507–515.

Y. WU ET AL, (1992) Computerized detection of clustered microcalcifications in digital mammograms: applications of artificial neural networks, Medical Physics., 19, 555–60.

Y. WU ET AL, (1993) Artificial neural networks in mammography: application to decision making in the diagnosis of breast cancer, Radiology, 187 (1), 81–7.

Received: June, 1997
Revised: March, 1998
Accepted: April, 1998

Contact address:
Thierry-Pascal Baum
3 Square Maryse Bastié
94310 Orly
France
e-mail: baum@ccr.jussieu.fr

THIERRY–PASCAL BAUM was born in Paris, France, in 1964. He received his State Medical Doctor Diploma in 1996 from the Paris XII University and his Ph.D. in medical informatics from the Paris VI University. His thesis concerned the detection of clusters of microcalcifications in digital mammograms. He obtained this thesis with distinction and with the examining board's utmost praise. He also studied in the United States where he received the Foreign Medical Graduate Examination in the Medical Sciences (FMGEMS), the Standard ECFMG Certificate, and the Federal Licensure Examination (FLEX).

His teaching activities concern practical work teaching in computer sciences in the 2nd year of college, Master of Electronic Imaging, and Master of Medical Informatics, at Paris V and Paris VI Universities. He is also giving lectures in Medical Informatics as part of the continuing education of hospital physicians at the Paris V University.

His research interests include medical informatics, biomedical imaging, multimedia and Web technologies, telemedicine, Internet, Intranet and Extranet architectures for hospitals, image storage and transmission, construction of a "Virtual University" for distance education through electronic networks.